Liquid-Loaded Piezo-Silicon Micro-Disc Oscillators for Pico-Scale Bio-Mass Sensing

Hakhamanesh Mansoorzare, *Graduate Student Member, IEEE*, Sarah Shahraini, *Member, IEEE*, Ankesh Todi, *Graduate Student Member, IEEE*, Nilab Azim, Swaminathan Rajaraman, *Member, IEEE*, and Reza Abdolvand, *Senior Member, IEEE*

***Abstract*— In this work, we report on the implementation of a closed-loop liquid-loaded resonant mass sensor as a test vehicle for the realization of highly sensitive miniaturized bio-marker assays. Using thin-film piezoelectric-on-silicon (TPoS) contour-mode disc resonators that are specifically designed and optimized for liquid-phase operation, a liquid-loaded low power (∼1.6 mW) oscillator at ∼17 MHz is demonstrated with a single transistor. By proper placement of the electrodes and the supporting tethers, a high liquid-loaded quality factor (∼380) and a low insertion loss (∼19 dB) are concurrently achieved which enable the accurate frequency tracking of the potential mass microbalance. The frequency shifts due to the liquid-loading and the preliminary characterized frequency stability of the oscillator imply a minimum mass detection resolution in the picograms range. [2020-0177]**

***Index Terms*— Liquid-loaded oscillator, liquid mass-sensing, microelectromechanical disc resonator, piezoelectric transducer.**

I. Introduction

OVERCOMING the global health issues calls for platforms that enable large scale testing and diagnosis as well as extensive drug and vaccine discovery. Such platforms require rapid, high throughput, and yet precise test vehicles that are capable of detecting specific biomarkers that often reside within a biological fluid. The enzyme-linked immunosorbent assay (ELISA) [1], is established as a clinical gold standard for detecting a diversity of biomarkers. However, ELISA in its conventional form, does not meet the aforementioned requirements and is considered to be resource intensive [2]. Therefore, enhancement of this scheme is desired, especially through automating the readout mechanism and miniaturizing the apparatus. In this regard, resonant sensors with a frequency output that could be directly interfaced with digital electronics are well suited. More specifically, piezoelectric resonators have been employed for sensing a variety of physical properties such as mass, density and viscosity since the establishment of the relationship between their adsorbed mass and resonance frequency. As of today, quartz crystal microbalances (QCM) invented by Sauerbrey remain one of the most widely used methods of accurate mass sensing [3]. Although, MEMS resonators offer miniaturization and integration beyond the limits possible with QCMs, utilization of such devices in liquid environment (i.e. biological media) has been rather limited. This is mainly because of the signal degradation that subsequently results in lower signal to noise ratio (SNR). The losses associated with the liquid-loading of the resonator are largely determined by its boundaries with the liquid and the mode-specific pattern of the radiation of energy into the liquid.

As such, we previously studied several resonance modes of liquid-loaded thin-film piezoelectric-on-silicon (TPoS) disc resonators to identify those with minimum quality factor (Q) degradation. Also the TPoS backside release step was modified to form a liquid-tight reservoir underneath the resonator by depositing a very thin (∼200 nm) layer of Parylene-C. Accordingly, a compound contour resonance mode with 4 nodal diameters and 2 nodal circles, conventionally named $S_{(4,2)}$, was identified to exhibit unprecedented liquid-phase Q [4]. Further, such resonators were embedded within a microfluidic testbed to prepare for the assembly of a closed-loop liquid-loaded sensing platform [5]. In this work, we have enhanced our earlier results by improving the coupling efficiency for the $S_{(4,2)}$ mode which has enabled implementation of a simple and low-power pierce oscillator for high resolution liquid-phase frequency tracking. From the results reported in this work the practical detection resolution limits that could be achieved using this system is estimated. The conceptual schematic of the proposed sensor is depicted in Fig. 1.

II. Design and Characterization of the Sensor

A. TPoS Disc Resonator

The electrode design guideline to achieve maximum coupling and minimum insertion loss (IL) in a TPoS resonator is to pattern the top electrode so that each connected piece of

Manuscript received May 15, 2020; revised July 3, 2020; accepted July 6, 2020. This work was supported by the National Science Foundation under Grant 1711632. The work of Swaminathan Rajaraman was supported by the University of Central Florida (UCF) Startup Funding. Subject Editor M. Rais-Zadeh. *(Corresponding author: Hakhamanesh Mansoorzare.)*

Hakhamanesh Mansoorzare, Sarah Shahraini, Ankesh Todi, and Reza Abdolvand are with the Department of Electrical and Computer Engineering, University of Central Florida, Orlando, FL 32816 USA (e-mail: hakha@knights.ucf.edu).

Nilab Azim is with the Department of Chemistry, University of Central Florida, Orlando, FL 32816 USA, and also with the NanoScience Technology Center, University of Central Florida, Orlando, FL 32816 USA.

Swaminathan Rajaraman is with the Department of Materials Science and Engineering, University of Central Florida, Orlando, FL 32816 USA, also with the Department of Electrical and Computer Engineering, University of Central Florida, Orlando, FL 32816 USA, and also with the NanoScience Technology Center, University of Central Florida, Orlando, FL 32816 USA.

Color versions of one or more of the figures in this article are available online at http://ieeexplore.ieee.org.

Digital Object Identifier 10.1109/JMEMS.2020.3008319

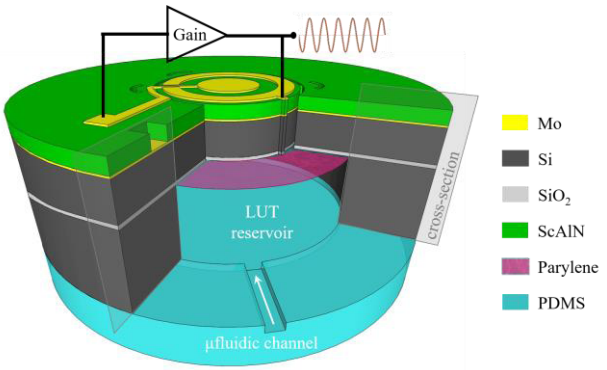

Fig. 1. The schematic of the MEMS microfluidic platform showing the TPoS resonator embedded within the LUT reservoir. Sustained oscillation is achieved by the addition of a simple electronic gain component.

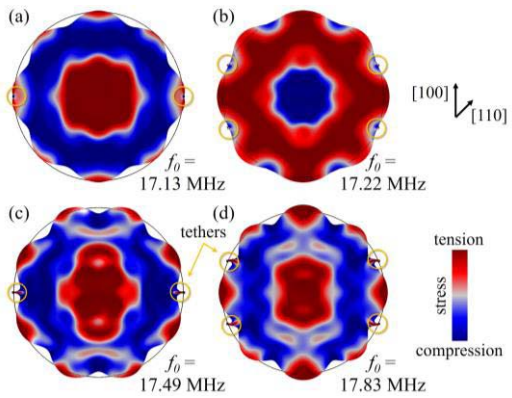

Fig. 2. (a), (b) The simulated lateral stress of the $S_{(4,2)}$ mode in a disc with radius of 400 μm and (c), (d) the spurious mode for two different clamping conditions.

conductor covers surface areas under which the stress polarity is similar. The lateral stress profile (vector sum of the stress in x and y direction) of the $S_{(4,2)}$ mode of a TPoS disc resonator with a radius of 400 μm is displayed in Fig. 2 (a) and (b). The former is clamped to the substrate from two spots along the [100] plane of silicon (Si) while the latter has four anchors along the 22.5° off [100] plane. Accordingly, two electrodes covering the opposite stress regions are considered. However, there exists a spurious mode that exhibits a stress pattern very similar to that of $S_{(4,2)}$ mode; as shown in Fig. 2 (c) and (d) respectively for the two clamping conditions. If not suppressed properly, this mode could cause unintended oscillations and false frequency tracking. Here we demonstrate that the clamping configuration with four anchors resolves such issue as for such design, all four tethers are located at maximum displacement node of the spurious mode as demonstrated in Fig. 2 (d) and substantially dampen the Q of the mode.

Two sets of TPoS disc resonators (DR) with a radius of 200 μm (DR_1) and 400 μm (DR_2) are fabricated on a stack of 1 μm scandium aluminum nitride ($Sc_{0.2}Al_{0.8}N$ provided by AMSystems Inc.) that is sandwiched between 100 nm thick molybdenum (Mo) electrodes and sputtered on a 16 μm silicon-on-insulator (SOI) substrate using a process flow that is elaborated in [5]. Liquid-phase operation is enabled once

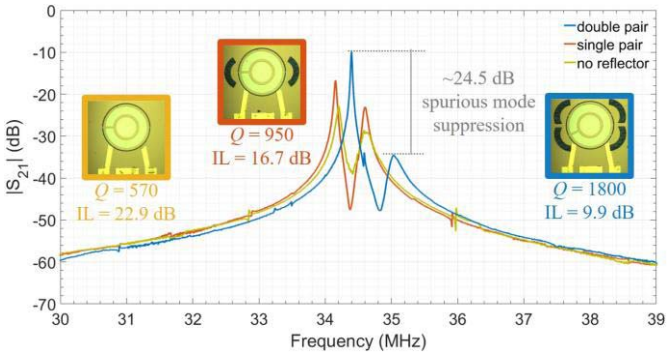

Fig. 3. Transmission response of DR_1 having different clamping and reflector configurations.

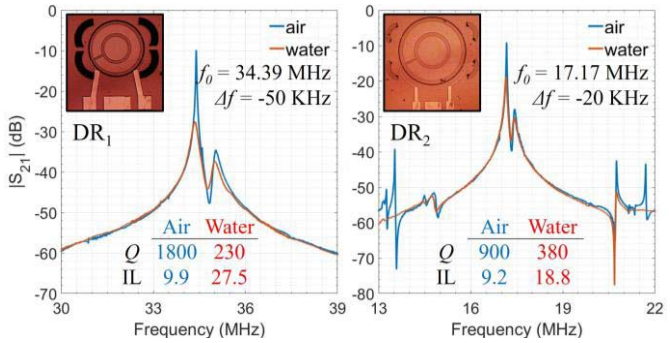

Fig. 4. Transmission response of DR_1 and DR_2 before and after insertion of DI water with the corresponding Q and IL.

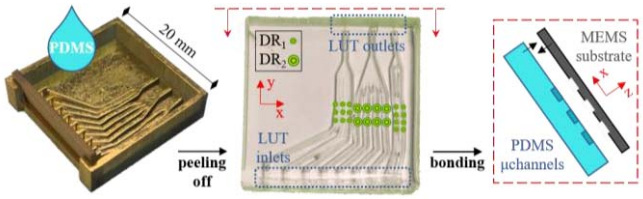

Fig. 5. Process flow for the integration of the microfluidics platform showing the PDMS casting, routing of formed microchannels (respective to DRs), and bonding of the PDMS structure underneath the MEMS substrate.

the resonators are embedded within a microfluidic device (elaborated in the following section) that is isolated from the resonator with a ~200 nm layer of Parylene-C. The insulating film is shortly treated with oxygen plasma to condition hydrophilic surfaces.

Prior to inserting the liquid under test (LUT), the RF characteristics of the disc resonators are measured by a Rohde & Schwarz ZNB 8 network analyzer. As expected and evidenced in Fig. 3, the four-anchor configuration exhibits superior performance (higher Q and lower IL) with ~24.5 dB suppression of the spurious mode. Additionally, the efficiency of utilizing in-plane acoustic reflectors [6], in such designs is evident. In the next step, the microfluidic channels are filled with deionized (DI) water and from the liquid-loaded responses, the sensitivity of the devices is determined. Fig. 4 displays the $|S_{21}|$ of DR_1 (34.39 MHz) and DR_2 (17.17 MHz) as well as their Q, extracted from their modified Butterworth-Van Dyke equivalent circuit, and IL before and after inserting

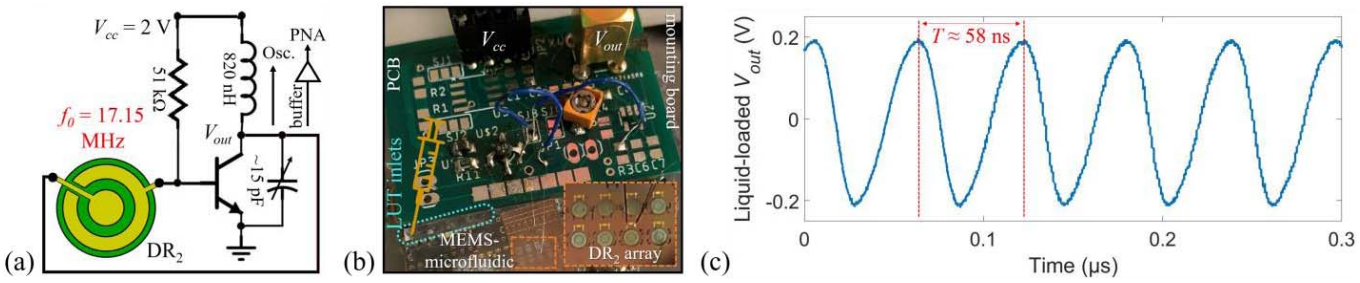

Fig. 6. (a) schematic of the single stage oscillator circuit; (b) the implemented oscillator circuit comprising the bonded MEMS-microfluidic along with the oscillator PCB; (c) the liquid-loaded output waveform of the oscillator.

DI water. Since the penetration of shear acoustic waves in the water approximately results in a virtual added mass [7] of 11.5 ng and 65 ng for DR_1 and DR_2, respectively, the measured liquid-loaded frequency shifts of 50 kHz and 20 kHz could be attributed to mass sensitivities of 128 ppm.ng^{-1} (4350 Hz.ng^{-1}) and 18 ppm.ng^{-1} (308 Hz.ng^{-1}), respectively. While DR_1 offers much higher mass sensitivity due to the smaller size and higher frequency, here, the preliminary oscillator is built with DR_2 as it offers substantially lower liquid-loaded IL and higher Q.

B. Microfluidic Platform

As an expandable platform for future implementation of a biomarker assay through functionalizing the Parylene-C layer with proper binding agents, arrays of disc resonators are integrated with the microfluidic channels. The microchannels that guide the LUT to the desired reservoirs underneath the resonators are fabricated using polydimethylsiloxane (PDMS)-based soft lithography. The process flow for the integration of the microfluidic structure is shown in Fig. 5. A 3D printed mold is sputtered with gold to enable easy detachment of the casted PDMS; the resulting cured structure is aligned with the MEMS substrate, so that the microchannels are properly routed underneath the resonators and the two are bonded to one another after a short oxygen plasma treatment.

C. Oscillator Circuit

The low liquid-loaded IL attained by DR_2 allows for implementation of the oscillator circuit with a single stage transistor-based sustaining amplifier. Consequently, a proof-of-concept pierce oscillator is demonstrated using a bipolar transistor (Avago's AT-41486 BJT) as schematically shown in Fig. 6 (a). The bonded MEMS-microfluidic substrate along with the oscillator's printed circuit board (PCB) are placed and secured on a mounting substrate (Fig. 6 (b)). The electrodes of the DR_2 are wire bonded to the circuit and DI water is injected into the LUT reservoir that is underneath DR_2 through the corresponding LUT microchannel inlet. The output waveform of the liquid-loaded oscillator (V_{out}) is displayed in Fig. 6 (c). With only 2 V supply voltage and 0.8 mA bias current the oscillator consumes 1.6 mW; considerably lower than the reported values in prior art [8]–[10].

Since the detection resolution of the sensor is governed by the frequency stability of the sensing oscillator, after insertion of an intermediate buffer stage, the liquid-loaded oscillator is characterized by a Rohde & Schwarz FSUP8 signal source analyzer; the measured phase noise and Allan deviation are plotted in Fig. 7 (a) and (b), respectively. While at a long sampling time (τ) prior to onset of random-walk, i.e. ~700-1000 s, the theoretical limit of frequency resolution (δf) is attainable, real-time mass sensing requires choosing small (<1 s) values of τ. Accordingly, δf at $\tau = 1$ s is estimated to be 1.5 Hz (9E-8 × 17.15 MHz); therefore, considering the derived mass sensitivity of 308 Hz.ng^{-1}, the mass resolution of the sensor is calculated to be 4.8 pg (1.5 Hz / 308 Hz.ng^{-1}) which as a reference is roughly four times the mass of a single Escherichia coli (E. coli) bacterium. As a side note, a confidence factor of ~3 is conventionally applied to the mass detection resolution to determine the limit of detection of the sensor (i.e. 14.4 pg).

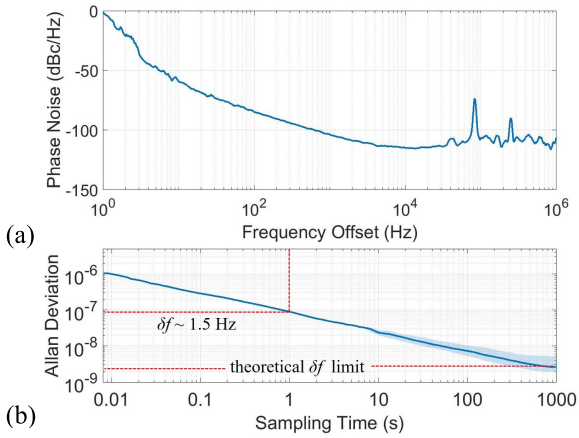

Fig. 7. Frequency stability characterization of the liquid-loaded oscillator showing the measured (a) phase noise and (b) Allan deviation; a frequency resolution of 1.5 Hz at $\tau = 1$ s sampling time is estimated.

III. Conclusion

A liquid-loaded MEMS microbalance platform was demonstrated that enables simple closed-loop operation for accurate readout. Future work would focus on functionalization of the microbalance with proper receptors for detection of biomarkers and single cell analysis within an assay.

References

[1] E. Engvall and P. Perlmann, "Enzyme-linked immunosorbent assay, ELISA: III. Quantitation of specific antibodies by enzyme-labeled anti-immunoglobulin in antigen-coated tubes," *J. Immunol.*, vol. 109, no. 1, pp. 129–135, 1972.

[2] S. O'Sullivan *et al.*, "Developments in transduction, connectivity and AI/Machine learning for point-of-care testing," *Sensors*, vol. 19, no. 8, p. 1917, Apr. 2019.
[3] G. Z. Sauerbrey, "Use of quartz vibrator for weighting thin films on a microbalance," *Zeitschrift Phys.*, vol. 155, no. 2, pp. 206–210, 1959.
[4] H. Mansoorzare, S. Moradian, and R. Abdolvand, "Parylene-coated piezoelectrically-actuated silicon disc resonators for liquid-phase sensing," in *Proc. 20th Int. Conf. Solid-State Sensors, Actuat. Microsyst. Eurosensors XXXIII (TRANSDUCERS EUROSENSORS XXXIII)*, Berlin, Germany, Jun. 2019, pp. 1207–1210.
[5] H. Mansoorzare *et al.*, "A microfluidic MEMS-microbalance platform with minimized acoustic radiation in liquid," *IEEE Trans. Ultrason., Ferroelectr., Freq. Control*, vol. 67, no. 6, pp. 1210–1218, Jun. 2020.
[6] H. Mansoorzare, S. Moradian, S. Shahraini, R. Abdolvand, and J. Gonzales, "Achieving the intrinsic limit of quality factor in VHF extensional-mode block resonators," in *Proc. IEEE Int. Freq. Control Symp. (IFCS)*, May 2018, pp. 1–4.
[7] L. McKenna, M. I. Newton, G. McHale, R. Lucklum, and J. Schroeder, "Compressional acoustic wave generation in microdroplets of water in contact with quartz crystal resonators," *J. Appl. Phys.*, vol. 89, no. 1, pp. 676–680, Jan. 2001.
[8] C.-H. Chiang, M.-C. Chou, P.-H. Hsieh, and M. S.-C. Lu, "Design and characterization of a CMOS MEMS capacitive oscillator for resonant sensing in liquids," *IEEE Sensors J.*, vol. 16, no. 5, pp. 1136–1142, Mar. 2016.
[9] C. Hadji, L. Virot, C. Picard, F. Baleras, and V. Agache, "MEMS with an embedded fluidic microchannel for sensitive weighing of liquid samples," in *Proc. IEEE 30th Int. Conf. Micro Electro Mech. Syst. (MEMS)*, Jan. 2017, pp. 1001–1004.
[10] S. Bhattacharya and S.-S. Li, "A fully differential SOI-MEMS thermal piezoresistive ring oscillator in liquid environment intended for mass sensing," *IEEE Sensors J.*, vol. 19, no. 17, pp. 7261–7268, Sep. 2019.